Analytical Sun Synchronous Low-Thrust Orbit Maneuvers

Stephanie Y. Docherty* and Malcolm Macdonald†

University of Strathclyde, Glasgow, G1 1XJ, Scotland, E.U.

Nomenclature

a	=	Semi-Major Axis (m)
c	=	Propulsion System Exhaust Velocity (m/s)
e	=	Eccentricity
i	=	Inclination (deg)
J_2	=	Dominant Earth Oblateness Term
m	=	Mass of spacecraft (kg)
$\dot{m}$	=	Mass Flow Rate of Low-Thrust Propulsion System (kg/s)
R	=	Mean Volumetric Radius of Earth (m)
r	=	Orbit Radius (m)
T	=	Spacecraft Thrust (N)
t	=	Time (Seconds)
Ω	=	Ascending Node Angle (deg)
$\dot{\Omega}$	=	Rate of Change of Ascending Node Angle (deg/s)
β	=	Out-of-plane Thrust Angle (deg)
ε	=	Acceleration of Spacecraft (m/s^2)
θ	=	True Anomaly (deg)
μ	=	Earth Gravitational Parameter (m^3/s^2)
σ	=	Order, of inferior order to

Subscripts

* Masters Student, Advanced Space Concepts Laboratory, stephanie.docherty@strath.ac.uk

† Associate Director, Advanced Space Concepts Laboratory, malcolm.macdonald.102@strath.ac.uk, Associate Fellow AIAA.

o = initial parameter value at time zero

f = final or target parameter value

I. Introduction

In general, the motion of a spacecraft under the influence of perturbations requires the application of numerical methods to interpret. However, adopting the assumption of a continuously acting force on a spacecraft in an initially circular orbit, with the continued absence of other perturbations, enables analytical solutions to be gained for some general problems.

In the absence of a spacecraft thrust vector it has long been established that consideration of non-Keplerian motion can generate useful orbit trajectories. For example, through careful consideration of the orbit perturbation force due to the oblate nature of the primary body, i.e. Earth, a secular variation of the ascending node angle of a near-polar orbit can be induced without expulsion of propellant, generating a so-called Sun-synchronous orbit. This was apparently first considered by Hanson and Fairweather [1] and recently extended using low-thrust propulsion to allow free selection of orbit altitude and inclination while maintaining a fixed ground-track by Macdonald et al. [2]. Following the work of Hanson and Fairweather, Brown considered the effect of the dominant Earth oblateness term, J_2, to enable orbit raising with continuous low-thrust propulsion in continuous sunlight, which was recognized as important to any solar power vehicle [3]. Subsequently, Ramler also considered Earth oblateness effects together with an out of orbit plane thrust to change the orbit inclination and ascending node angle [4]. The analysis of Brown and Ramler was then generalized analytically by M^{c}Innes for terminally unconstrained orbit raising [5, 6].

Herein, the previous work considering terminally unconstrained orbit raising is extended to develop an analytical solution of low-thrust orbit transfers between Sun-synchronous orbits. A validation of this analytical approach is also presented using numerical analysis and further optimization. It is explicitly noted that, while existing work largely considers problems in which only the initial conditions are specified, the methods used in this work allow for solution of the two point boundary transfer problem between Sun-Synchronous orbits. While numerical methods alone could be used to solve such problems, the use of an accurate analytical method significantly reduces the time required to find a solution, along with the computational load of doing so, by rapidly providing a high-quality initial solution.

II. Orbit Dynamics

A low-thrust orbit raising maneuver from an initially, or nearly circular orbit, using tangential thrusting can be approximated as a quasi-circular spiral [7] and as such the orbit radius, r, is used to replace the semi-major axis, assuming that eccentricity is negligible. Note that with tangential thrusting although the instantaneous variation in eccentricity is non-zero, the secular variation of eccentricity is zero. It is noted from Eq. (1) that any component of thrust which is out of the orbit plane will not contribute towards the orbit raising maneuver as only in-plane thrusting alters the rate of change of orbit semi-major axis. Resultantly, within this analytical analysis, the spacecraft thrust is directed along the vehicle tangential direction and pitched at an angle β out of the orbit plane, as shown in Fig. 1, such that the orbit energy and plane can be controlled. The radial component of acceleration is thus zero. The Lagrange-Gauss variational equations for semi-major axis, inclination, ascending node, and true anomaly, [8] become,

$$\frac{dr}{dt} = \frac{da}{dt} = \frac{2}{\sqrt{\mu}} \frac{T}{m(t)} \cos\beta \, a^{\frac{3}{2}} \tag{1}$$

$$\frac{di}{dt} = \frac{T}{m(t)} \sin\beta \cos\theta \sqrt{\frac{a}{\mu}} \tag{2}$$

$$\frac{d\Omega}{dt} = \frac{T}{m(t)} \sin\beta \frac{\sin\theta}{\sin i} \sqrt{\frac{a}{\mu}} - \frac{3}{2} \frac{\bar{n} J_2 {R_\oplus}^2 \cos i}{a^2} \tag{3}$$

$$\frac{d\theta}{dt} = \sqrt{\frac{\mu}{a^3}} \tag{4}$$

where,

$$\bar{n} = \sqrt{\frac{\mu}{a^3}} + \mathcal{O}(J_2) \tag{5}$$

$$m(t) = m_0 - \dot{m}t \tag{6}$$

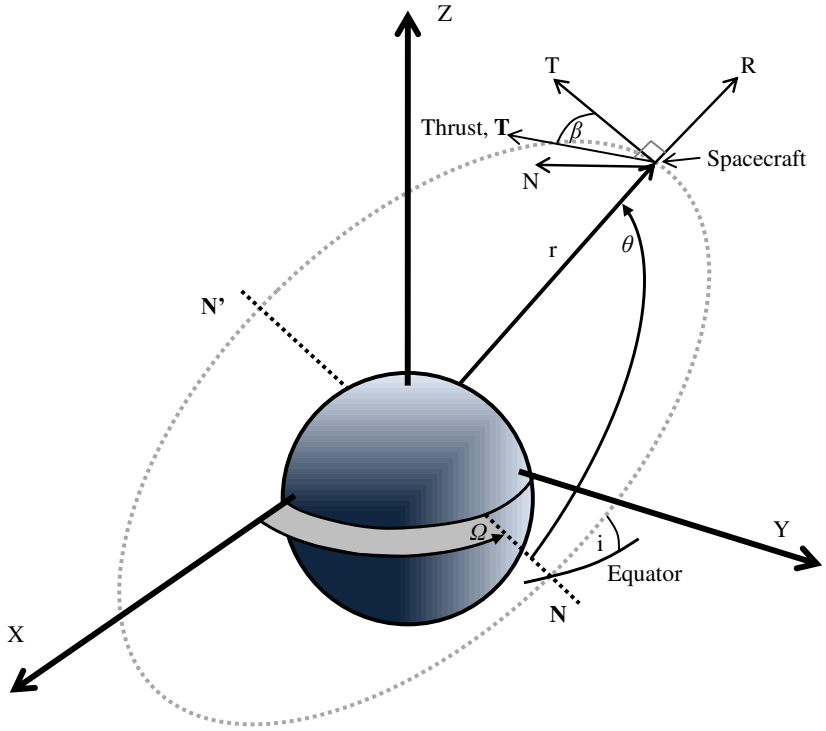

Fig. 1 Orbit geometry with ascending node N and descending node *N'* and thrust induced acceleration orientation

The Lagrange-Gauss variational equations may be averaged with respect to true anomaly to obtain the long-period motion using the averaging operator,

$$\langle z \rangle = \frac{1}{2\,\pi}\int_0^{2\pi} z\; d\theta \tag{7}$$

gaining,

$$\langle \frac{da}{dt} \rangle = \frac{a^{\frac{3}{2}}}{\pi\sqrt{\mu}}\frac{T}{m(t)}\int_0^{2\pi} \cos\beta\;(\theta)\; d\theta \tag{8}$$

$$\langle \frac{di}{dt} \rangle = \frac{1}{2\pi}\frac{T}{m(t)}\sqrt{\frac{a}{\mu}}\int_0^{2\pi} \sin\beta\cos\theta\;(\theta)\; d\theta \tag{9}$$

$$\langle \frac{d\Omega}{dt} \rangle = \frac{1}{2\pi\sin i}\frac{T}{m(t)}\sqrt{\frac{a}{\mu}}\int_0^{2\pi} \sin\beta\sin\theta\;(\theta)\; d\theta - \frac{3}{2}\frac{\sqrt{\mu}\,J_2\,{R_\oplus}^2\cos i}{a^{\frac{7}{2}}} \tag{10}$$

It should be noted that the use of orbit averaging to obtain long-period motion means that any orbit maneuver will only be accurately represented over an integer number of revolutions. This anomaly will be increasingly prominent for short orbit transfers, where the short-period variations represent a more significant fraction of the total orbit maneuver magnitude.

A. Constant Acceleration

For a spacecraft with low-thrust propulsion, such as a Solar Electric Propulsion (SEP) system, the reduction in spacecraft mass due to exhaust gases may, in-general, be neglected for short duration maneuvers. As such systems generally maintain constant thrust, this leads the initial acceleration, ε_0, to remain constant. Eq. (8) – (10) may be re-written using Eq. (11) [9, 10] and assuming zero mass change with respect to time.

$$\frac{T}{m(t)} = \frac{\varepsilon_0}{1 - \frac{\varepsilon_0}{c} t} \tag{11}$$

Thereafter, the modified Eq. (8) – (10) can be solved by defining an out-of-plane thrust angle profile with respect to true anomaly. From Eq. (2) it can be seen that for a fixed angle β ($\neq {}^{\pi}/_{2}$) the rate of change inclination will switch sign at true anomaly (${}^{\pi}/_{2}$) and (${}^{3\pi}/_{2}$). Therefore, by switching the out-of-plane thrust vector orientation in accordance with this variation, a uniformly positive or negative variation in inclination can be gained [11, 12]. Eq. (8) is thus solved directly to obtain,

$$a(t) = \frac{a_0}{\left(1 - \varepsilon_0 \cos\tilde{\beta} \sqrt{\frac{a_0}{\mu}} t\right)^2} \tag{12}$$

where, $\tilde{\beta}$ switches between $\{-\beta, +\beta\}$ every half-orbit at true anomaly (${}^{\pi}/_{2}$) and (${}^{3\pi}/_{2}$). Eqs. (9) and (10) can thereafter be solved sequentially to obtain,

$$i(t) = i_0 + \kappa\zeta \tag{13}$$

$$\Omega(t) \tag{14}$$

$$= \Omega_0$$

$$+ \frac{3}{2} \frac{J_2}{\varepsilon \cos\tilde{\beta}} \frac{\mu}{a_0^2} \left(\frac{R_\oplus}{a_0}\right)^2 \frac{\{\exp(8\zeta)\,[8\cos(\kappa\zeta + i_0) + \kappa \sin(\kappa\zeta + i_0)] - (8\cos i_0 + \kappa \sin i_0)\}}{64 + \kappa^2}$$

where,

$$\zeta = \log\left(1 - \varepsilon\cos\tilde{\beta}\sqrt{\frac{a_0}{\mu}}t\right) \tag{15}$$

$$\kappa = -\left(\frac{2}{\pi}\right)\tan\tilde{\beta} \tag{16}$$

Note that Eqs. (12) and (13) match those previously derived in [6], while Eq. (14) corrects a typo in the same.

B. Constant Thrust

The derivation of Eqs. (12) – (14) assumed that a constant acceleration was delivered by the low-thrust propulsion system. However, this result can be extended to consider constant thrust from the low-thrust propulsion system, where reduction in spacecraft mass due to exhaust gases is no longer neglected, hence providing a more accurate solution. Using Eq. (11) for only constant thrust to rewrite Eq. (8) and subsequently solving gives,

$$a(t) = \frac{a_0}{\left[1 + \cos(\tilde{\beta})\, c\sqrt{\frac{a_0}{\mu}}\log\left(1 - \frac{\varepsilon_0}{c}t\right)\right]^2} \tag{17}$$

where, $\tilde{\beta}$ switches between $\{-\beta, +\beta\}$ every half-orbit. Similarly, Eq. (9) can thereafter be solved to obtain,

$$i(t) = i_0 + \kappa\varphi \tag{18}$$

where, κ is as shown in Eq. (16), and

$$\varphi = \log\left[1 + c\sqrt{\frac{a_0}{\mu}}\cos\tilde{\beta}\log\left(1 - \frac{\varepsilon_0 t}{c}\right)\right] \tag{19}$$

Finally, the ascending node angle may be obtained from Eq. (10) using Eqs. (17) and (18),

$$\Omega(t) = \Omega_0 + \frac{3}{2}\frac{J_2}{\varepsilon_0\cos\tilde{\beta}}\frac{\mu}{a_0^2}\left(\frac{R_\oplus}{a_0}\right)^2\left(1 - \frac{\varepsilon_0}{c}t\right)\int_{\varphi_0}^{\varphi_1} exp(8\varphi)\cos(i_0 + \kappa\varphi)\, d\varphi \tag{20}$$

It can thereafter be found that Eq. (20) can be solved to obtain,

$$\Omega(t) = \Omega_0 + \frac{3}{2}\frac{J_2}{\varepsilon\cos\tilde{\beta}}\frac{\mu}{a_0^2}\left(\frac{R_\oplus}{a_0}\right)^2\Big(1 - \frac{\varepsilon_0}{c}t\Big)\frac{\{\exp(8\varphi)\,[8\cos(\kappa\varphi + i_0) + \kappa\sin(\kappa\varphi + i_0)] - (8\cos i_0 + \kappa\sin i_0)\}}{64 + \kappa^2} \tag{21}$$

For both constant thrust and constant acceleration, these sets of closed-form analytical equations can henceforth be used not only to predict the spacecraft trajectory but also to control the spacecraft trajectory, enabling the continuous, low-thrust two-point boundary value trajectory transfer problem to be solved analytically.

III. Analytical Sun-Synchronous Orbit Transfers

Consider a two-point boundary transfer problem between an initial and target Sun-synchronous orbit. In order to obtain a standard Sun-synchronous orbit, the orbit inclination must be equal to [2],

$$i = \cos^{-1}\left[-\frac{2}{3}\frac{\dot{\Omega}ss}{J_2}\frac{a^{7/2}(1-e^2)^2}{{R_\oplus}^2\sqrt{\mu}}\right] \tag{22}$$

where, $\dot{\Omega}ss$ is the mean rotation rate of the Sun within an Earth-centered inertial reference frame per second i.e. equal to 360/365.24 = 0.986 degrees per day.

A. Sun-synchronous to Sun-synchronous Transfer with Constant Acceleration

For an initially Sun-synchronous orbit, and assuming at all times that the trajectory remains nearly circular, the initial inclination i_o will be equal to the inclination as shown in Eq. (22), where a will be equal to the initial semi-major axis a_o. For the final orbit to be Sun-synchronous, the final inclination, i_f, must also be defined by Eq. (22) where a will be equal to the target semi-major axis a_f. Therefore, this target semi-major axis can be equated to the semi-major axis as in Eq. (12), where t_f will represent the transfer duration,

$$a_f = \frac{a_0}{\left(1-\varepsilon\cos\tilde{\beta}\,\sqrt{\frac{a_0}{\mu}}t_f\right)^2} \tag{23}$$

Similarly, the target inclination can be equated to the inclination shown in Eq. (13) as,

$$i_f = \cos^{-1}\left[-\frac{2}{3}\frac{\dot{\Omega}ss}{J_2}\frac{{a_f}^{7/2}(1-e^2)^2}{{R_\oplus}^2\sqrt{\mu}}\right] \tag{24}$$

$$= i_0 - \left(\frac{2}{\pi}\right)\tan\tilde{\beta}\log\left(1-\varepsilon\cos\tilde{\beta}\,\sqrt{\frac{a_0}{\mu}}t_f\right)$$

Thus, using Eq. (23) and (24), the transfer can be solved analytically for values of the required out-of-plane thrust angle $\tilde{\beta}$ and transfer duration t_f by finding the appropriate root of the system. Furthermore, as Eq. (22) directly incorporates the required mean rate of change of the ascending node angle, the actual ascending node angle can be expected to naturally rotate, due to J_2, during the orbit transfer such that not only will the Sun-Synchronous condition be maintained at all times, but the relative orientation of the orbit normal and Sun-line should also remain constant.

B. Sun-synchronous to Sun-synchronous Transfer with Constant Thrust

A similar manipulation of equations can be carried out on those which represent a constant thrust transfer. The procedure is as described for constant acceleration, however in this case the target semi-major axis, a_f, is equated to the semi-major axis as shown in Eq. (17),

$$a_f = \frac{a_0}{\left[1 + \cos(\tilde{\beta})\, c \sqrt{\frac{a_0}{\mu}} \log\left(1 - \frac{\varepsilon_0}{c} t_f\right)\right]^2} \tag{25}$$

Similarly, the target inclination is equated to the inclination shown in Eq. (18),

$$i_f = \cos^{-1}\left[-\frac{2}{3}\frac{\dot{\Omega}\mathrm{ss}}{J_2}\frac{{a_f}^{7/2}(1-e^2)^2}{{R_\oplus}^2\sqrt{\mu}}\right] \tag{26}$$

$$= i_0 - \left(\frac{2}{\pi}\right)\tan\tilde{\beta}\log\left[1 + c\sqrt{\frac{a_0}{\mu}}\cos\tilde{\beta}\log\left(1 - \frac{\varepsilon_0 t_f}{c}\right)\right]$$

Again, in this case using Eq. (25) and (26), this transfer can be solved analytically for values of the required out-of-plane thrust angle $\tilde{\beta}$ and transfer duration t_f by finding the appropriate root of the system. Once again, as this remains a Sun-synchronous to Sun-synchronous transfer, the Sun-synchronous orbit alignment can be expected to be maintained at all times.

IV. Numerical Validation of Analytical Analysis

In order to assess the validity of the general perturbations solution, a special perturbations solution is generated using the analytically generated control profile, i.e. the transfer time and the out of plane angle, $\tilde{\beta}$; the terms general and special perturbations are defined in [13]. As described in section II A, $\tilde{\beta}$ must switch between $\{-\beta, +\beta\}$ every half-orbit at true anomaly ($^{\pi}/_{2}$) and ($^{3\pi}/_{2}$) in order to maintain a uniformly positive, or negative, variation in inclination. The special perturbations analysis therefore assumes that the normal component of acceleration direction varies as a step, moving from positive to negative every half orbit, while the tangential component of acceleration direction remains constant and the radial component of acceleration direction is always equal to zero. This special perturbations technique numerically propagates the spacecraft position by integration of the modified equinoctial equations of motion in the Gauss' form [14, 15]. This is done using an explicit, variable step-size Runge-Kutta (4, 5) formula, the Dormand-Prince pair (a single step method) [16].

The result of the special perturbations analysis is thereafter used as an initial guess to allow numerical optimization of the spacecraft control profile to quantify the optimality of the general perturbations solution.

Numerical optimization is conducted using a Pseudospectral Optimal Control Solver (PSOPT) which once again propagates the spacecraft position using modified equinoctial equations of motion in the Gauss' form [17, 18]. PSOPT[‡] is an open source optimal control software package written in C++ that uses direct collocation methods, including pseudospectral and local discretizations to solve optimal control problems [19]. The numerical optimization objective function was, at all times, to maximize the final spacecraft mass, that is to say, to minimize the propellant required.

Consider a transfer between two circular Sun-synchronous orbits, with an initial acceleration of 1 mm/s^2, an initial spacecraft mass of 500 kg, and a specific impulse of 3000 seconds. The initial orbit is assumed to be similar to that of ENVISAT i.e. a repeat ground-track after 501 revolutions over 35 days, with an initial altitude of 781 km and an initial inclination of 98.52 degrees. The control profile for an orbit transfer to a Sun-synchronous orbit with a 30 km higher altitude can be analytically determined by finding the roots of the system as discussed in III A and III B for constant acceleration and constant thrust respectively. Using special perturbations techniques to propagate each analytically determined transfer trajectory, it is found that the transfer time decreases slightly in both cases due to the orbit averaging technique applied in the general perturbations method. The given special perturbations solution can then be used as an initial guess such that the transfer can be numerically optimized, while maintaining the constraint that the radial acceleration equals zero at all times.

Table 1 displays the general and special perturbations solutions, and the numerically optimized solution for both constant acceleration and constant thrust. It can be noted that in the case of constant thrust, as acceleration is no longer constant, the final mass produced by the general perturbations solution can be calculated using Eq. (11).

[‡] See also www.psopt.org, cited 26 January 2011.

Table 1 General and special perturbations, and numerically optimized solutions for constant acceleration and constant thrust

	Constant Acceleration	Constant Thrust
General Perturbations Solution		
Required Out of Plane Thrust Angle, deg	58.9	58.9
Transfer Time, s	30414	30602
Final Mass, kg	500	499.48
Fuel Requirement, kg	N/A	0.52
Special Perturbations Solution		
Transfer Time, s	30285	30286
Final Mass, kg	499.49	499.49
Fuel Requirement, kg	0.51	0.51
Numerically Optimized Solution		
Transfer Time, s	29922	29940
Final Mass, kg	499.49	499.49
Fuel Requirement, kg	0.51	0.51

The general perturbations solution is found to have provided a high-quality initial guess, with a transfer time inaccuracy of only 1.7 % for constant acceleration and 2.2% for constant thrust, in comparison with the optimized solution. It can be seen that, in the presented case of constant thrust, the general perturbation solution is practically fuel optimal, with an additional fuel requirement of only 0.01 kg, 0.002% of the initial spacecraft mass. Optimization of the spacecraft control profile for the case of constant acceleration is as shown in Fig. 2.

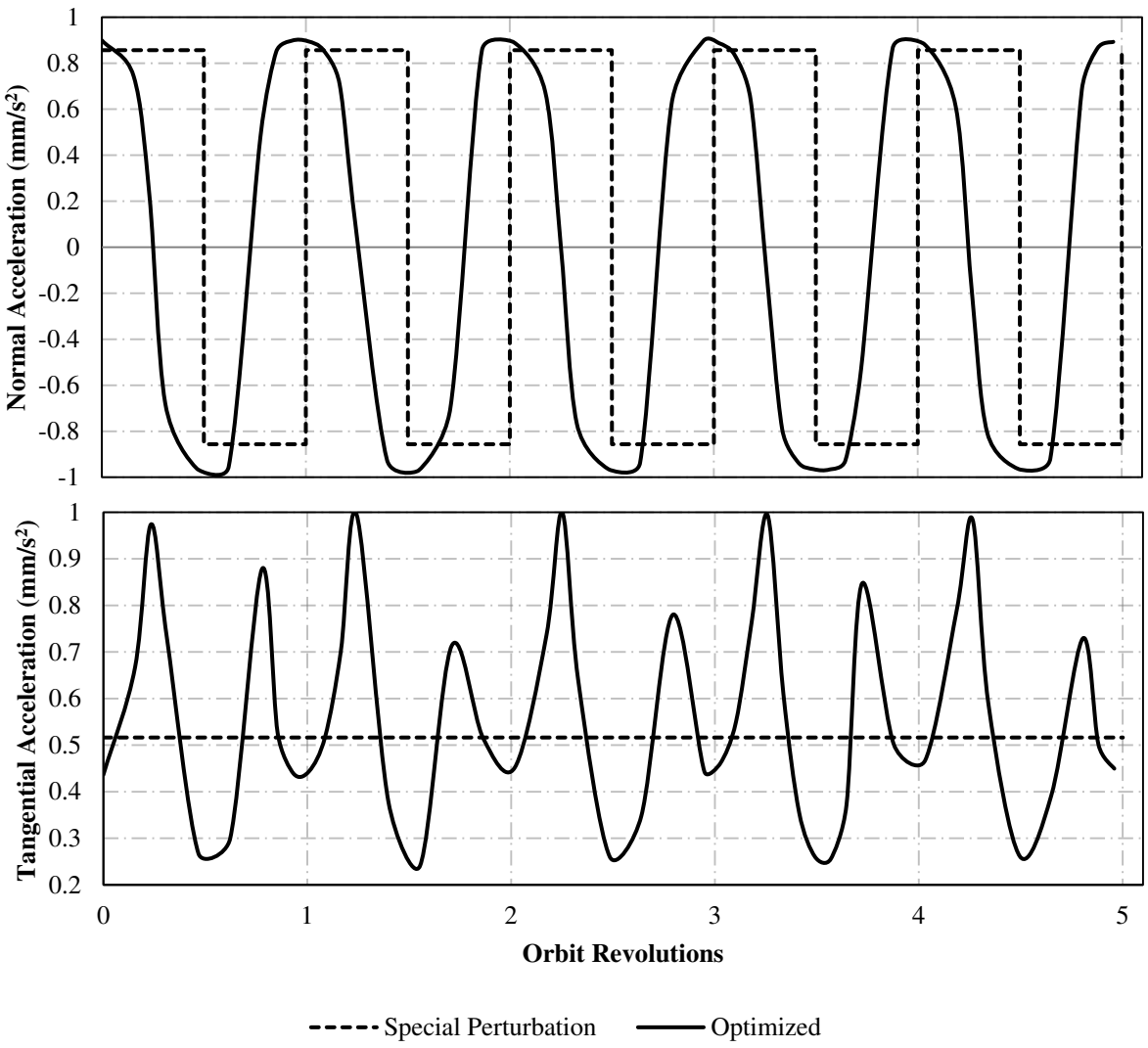

Fig. 2 Variation of normal (top) and tangential (bottom) control acceleration for a Sun-synchronous to Sun-synchronous transfer with constant propulsive acceleration

Considering the special perturbations solution, the times at which the normal control profile switches direction, represented by the sharp corners in Fig. 2, are essentially times where the engine is continuing to thrust yet the acceleration is having very little, or no effect on the spacecraft trajectory. This can be understood by considering Eq. (2), where the cosine term will force zero rate of change of the ascending node when the true anomaly is ($\pi/2$) and ($3\pi/2$), corresponding to the switching profile of the control law. Therefore, the use of a numerical optimizer eliminates inefficient use of propellant by smoothing the control profile for the normal acceleration around these areas. Consequently, due to the optimizer's variation in out-of-plane thrust magnitude, the tangential acceleration

magnitude is also no longer constant, varying in phase with the normal acceleration with approximately one oscillation per half-orbit revolution. For the case of constant thrust, the special perturbations and numerically optimized control profiles for both the normal and tangential components of acceleration appear almost identical to that shown in Fig. 2. It should be noted that in this case, the magnitude of the total acceleration will increase due to the reduction in spacecraft mass; however this increase is only marginal and hence is not clearly evident.

The optimized numerical transfer altitude and inclination variation can be compared with that of the general and special perturbations transfers, as shown in Fig. 3 for the case of constant acceleration.

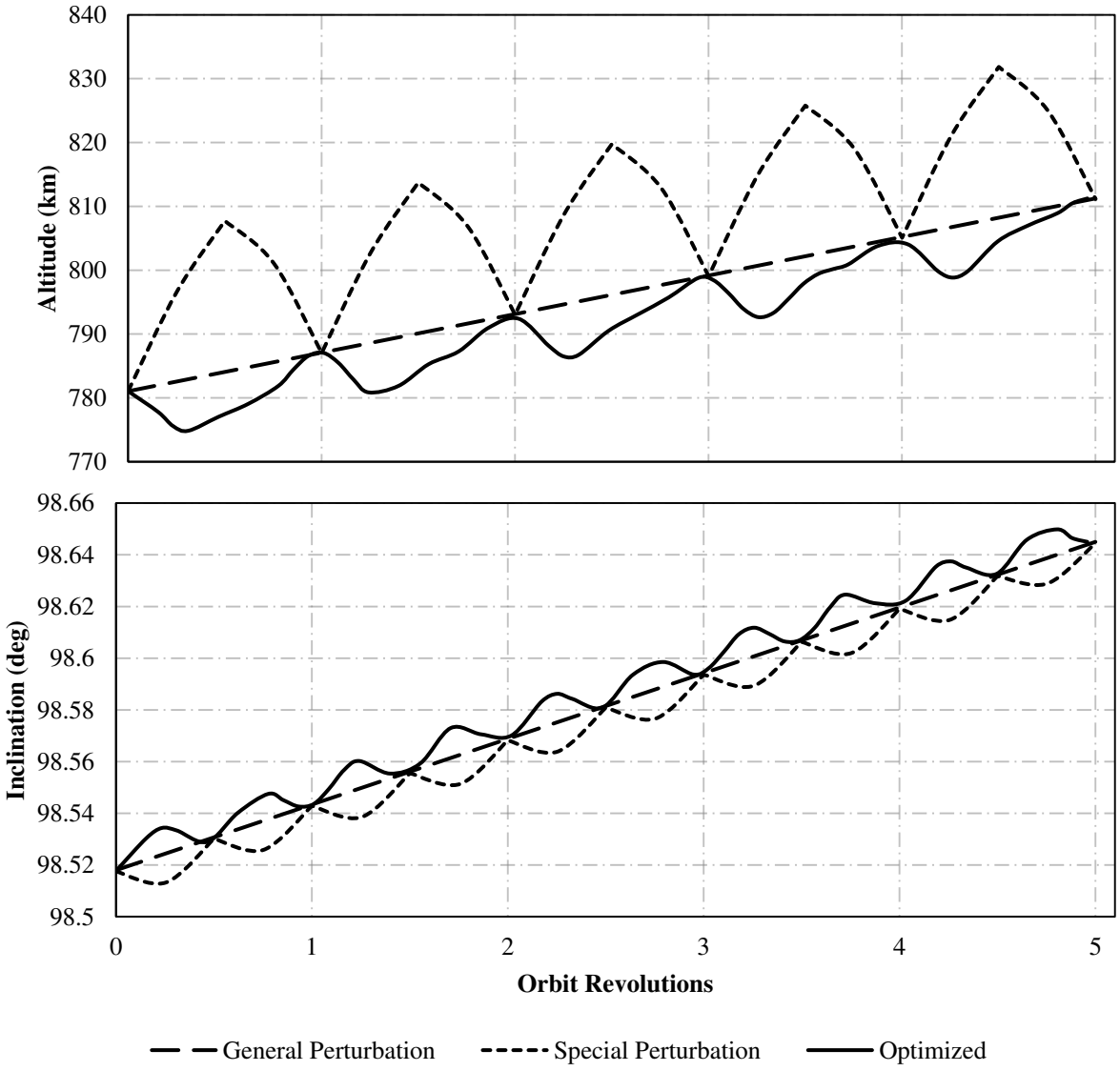

Fig. 3 Variation of altitude (top) and inclination (bottom) due to the control profile shown in Fig. 2

In terms of altitude variation shown in Fig. 3, the special perturbations solution and the numerically optimized solution oscillate over one orbit revolution. The troughs of the special perturbations solution and peaks of the numerically optimized solution coincide with each other, and the general perturbations solution, after each revolution, and thus the increase in orbit altitude is occurring at the same steady rate for all solutions. The variation of inclination in Fig. 3 has a behavior similar to that of altitude, only with oscillation occurring twice over one revolution. Again, the inclination is increasing at the same steady rate for all solutions. It can therefore be deduced that the analytical representation of the transfer is representing the given transfer to a high-level of agreement. For constant thrust, the variation of altitude and inclination for all three solutions appear almost identical to those shown in Fig. 3 and hence are not represented.

As discussed previously, it is anticipated that a transfer between two Sun-synchronous orbits will maintain a constant alignment to the Sun. Thus, the rate of change of the right ascension of the ascending node, equal to $\dot{\Omega}_{SS}$, should remain relatively steady at 0.986 degrees per day. With a constant rate of change, the desired value of the ascending node angle will increase linearly during numerical optimization. Although the variation of the ascending node angle for the numerically optimized solution was found to increase almost linearly, small oscillations occur around the desired linear variation, with, as expected from Eq. (3), approximately two oscillations per revolution. This can be observed by considering the difference between the ascending node angle for the optimized solution and the desired ascending node angle, shown in Fig. 4 for the case of constant acceleration, and appears almost identical for the case of constant thrust.

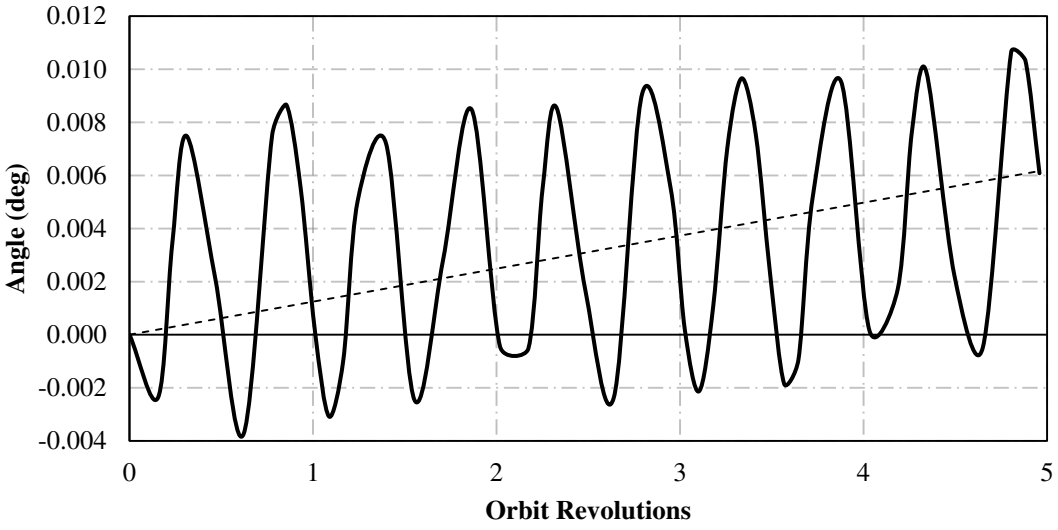

Fig. 4 Difference between ascending node angle for optimized transfer and desired ascending node angle (−) and associated linear trendline (- -) for a Sun-synchronous to Sun-synchronous transfer with constant propulsive acceleration

On average, the difference between the optimized ascending node angle and the desired ascending node angle increases by 1.2 millidegrees per orbit revolution. Thus over the full transfer, the optimized ascending node angle has an average error of 6 millidegrees with respect to the desired ascending node angle. This can be compared with the general perturbations solution which, over the duration of the transfer, was found to have an error of only 0.014 millidegrees. It can be noted that, in general, the differences between the constant acceleration and constant thrust solutions are small and thus the assumption of constant acceleration is valid for such short transfers. This was also found for transfers of varying initial mass, specific impulse, and altitude change.

As anticipated, due to the orbit averaging technique applied, the general perturbations solution does not represent the oscillation of the orbital elements such as altitude and inclination. This can be understood by examination of Fig. 2, for example a transfer of 4.5 orbit revolutions would result in a considerable difference in altitude between the general perturbations and both the special perturbations and numerically optimized solutions.

Removing Constraint on Radial Acceleration

Consider once again the constant thrust transfer, however now removing the constraint during numerical optimization on the radial component of acceleration to equal zero at all times, as assumed in the general

perturbations solution. The transfer time is found through numerical optimization to be very similar to that of the constrained solution, in this case, being reduced from 29940 seconds to 29934 seconds. The final mass of the spacecraft also remains the same at 499.49 kg. The normal acceleration solution is found to be extremely similar to that of the no radial acceleration solution, while for the tangential component of acceleration the pattern of two oscillations per orbit revolution in-phase with the normal component of acceleration remains. The radial component of acceleration also varies in phase with the normal acceleration, with approximately one oscillation per orbit revolution. Although allowed to vary, the maximum magnitude of the radial acceleration is only approximately 0.08 mm/s^2. This small magnitude results in a very similar variation of normal and tangential acceleration to the constrained transfer. The variation of all components of acceleration, radial, normal, and tangential, is shown in Fig. 5.

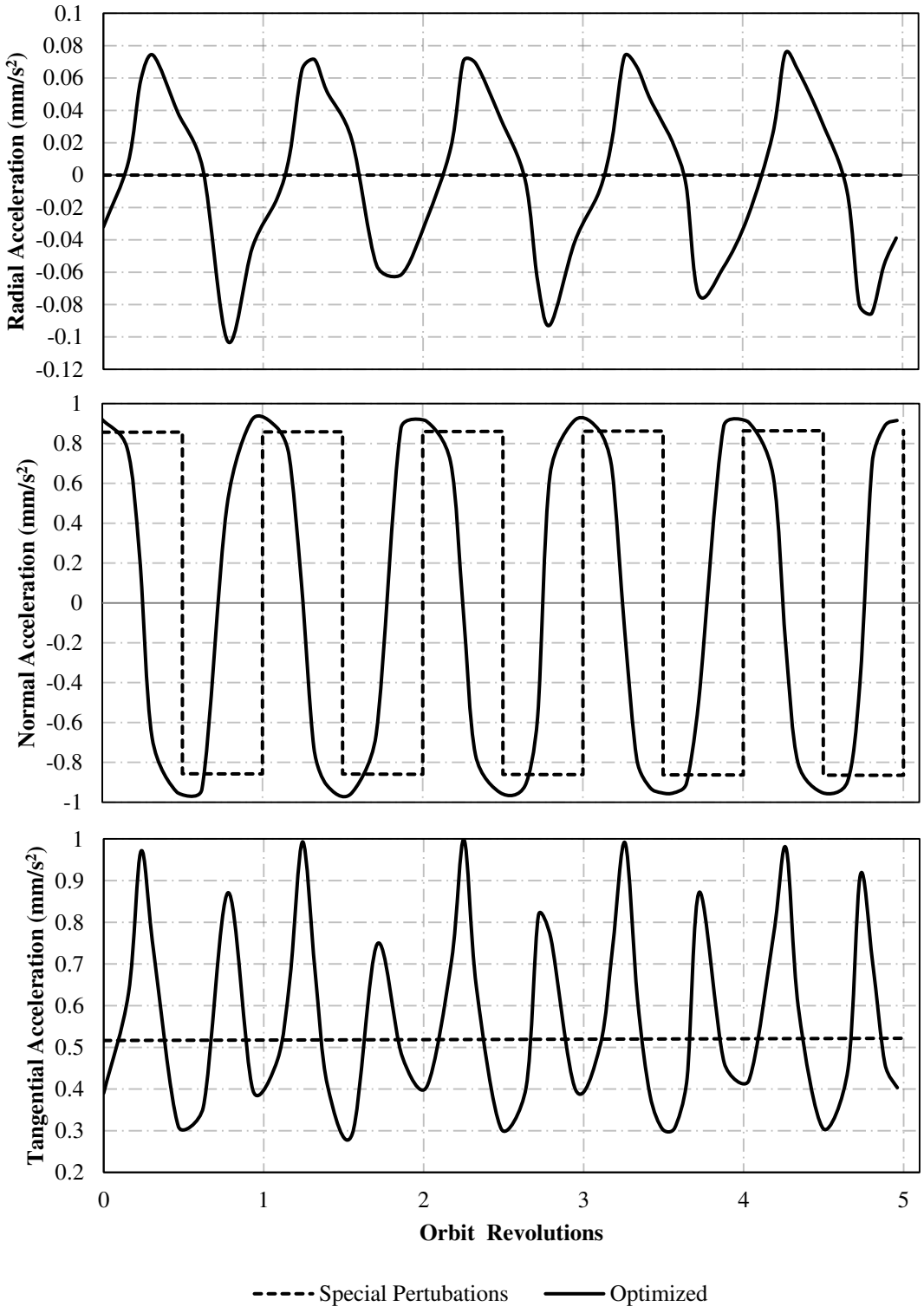

Fig. 5 Variation of Radial (top), Normal (middle), and Tangential (bottom) Acceleration for a Sun-synchronous to Sun-synchronous transfer with constant thrust

Removing this constraint on the radial acceleration was found to have very little effect on the variation on the ascending node angle. And as for the constrained transfer, that is, without radial thrusting, the variation of altitude and inclination were shown to be very similar to that in Fig. 3.

V. Discussion

It is noted that, in this work, the example transfer presented is a very short time transfer with an altitude change of only 30 km. While the general perturbations technique used could obtain a solution for a transfer of considerably larger magnitude, limitations of the numerical solver used to attain the optimal solution presented restrictions in the maximum altitude change with which optimality could be examined.

Use of the general perturbations technique derived here on-board a spacecraft would significantly reduce complexity of spacecraft control in comparison with the use of the optimal solution, hence reducing the possibility of error. The solution provides a straightforward analytical control law for transfers between Sun-synchronous orbits, potentially suitable for use on an autonomous craft, unlike the fully optimised solution. As well as reduced complexity of spacecraft operations, spacecraft design could also be simplified by use of the analytical control profile derived from the general perturbations solution which would require only an on/off thrusting capacity. Use of the control profile generated by the numerical optimizer would however necessitate a very highly controlled thrust vector in the form of either a steerable thrust vector, or continuously throttled thrust magnitudes on several thrusters. Use of the general perturbations analysis can hence provide significant advantages in terms of practicality with almost no penalty in optimality. Although a comprehensive robustness check has not be performed in this work, it was found that the inclusion of additional perturbation terms J_3 and J_4 had negligible effect on the practicality of the solution method.

VI. Conclusions

A general perturbations representation of a two-point boundary value transfer between two sun-synchronous orbits has been achieved for both constant acceleration and constant thrust. Validation of this general perturbations solution was achieved through the use of special perturbations and numerical optimization. Maintaining an objective function to minimize propellant use, the general perturbations solution for constant thrust was found to be very nearly optimal in terms of mass consumption. The transfer time of the general perturbations solution was found to be accurate to within less than two percentage points with respect to the numerically optimized solution.

VII. References

1 Hanson, J.N., Fairweather, S.H,, "Nodal Rotation for Continuous Exposure of an Earth Satellite to the Sun", Journal of the American Rocket Society, Vol. 31, No. 5, pp. 640 – 645, 1961.

2 Macdonald, M., McKay, R., Vasile, M., Bosquillon de Freschville, F., "Extension of the Sun-Synchronous Orbit", Journal of Guidance, Control, and Dynamics, Vol. 33, No. 6, pp 1935– 1940, 2010.

3 Brown, D.W., "Low-Thrust Orbit Raising in Continuous Sunlight", NASA TN D-2072, 1964.

4 Ramler, J.R., "Low-Thrust Orbit Raising in Continuous Sunlight while Thrusting in a Plane Perpendicular to the Earth-Sun Line", NASA TN D-4104, 1967.

5 McInnes, C.R., "Low-Thrust Orbit Raising with J2 Regression", The Aeronautical Journal, Vol. 101, No. 1007, pp. 295 – 298, 1997.

6 McInnes, C.R., "Low-Thrust Orbit Raising with Coupled Plane Change and J2 Precession", Journal of Guidance, Control and Dynamics, Vol. 20, No. 3, 1997, pp. 607 – 609.

7 Vallado, D., "Fundamentals of Astrodynamics and Applications", Microcosm Press, Hawthorne, CA, 2007, pp.377 – 383.

8 Roy, A.E., "Orbital Motion", Taylor & Francis Group, LLC, Abingdon, Oxon, U.K., 2005, pp. 208 – 220.

9 Wakker, K.E., "Rocket Propulsion and Spaceflight Dynamics", Pitman, London, 1984, pp. 462 – 479.

10 Wiesel, W.E., "Spaceflight Dynamics", McGraw-Hill, New York, 1991, pp. 89 – 91.

11 Macdonald M., McInnes C. R. "Analytical Control Laws for Planet-Centred Solar Sailing", Journal of Guidance, Control and Dynamics, Vol. 28, No. 5, 2005, pp 1038 – 1048.

12 Macdonald M., M^{c}Innes C. R., Dachwald, B., "Heliocentric Solar Sail Orbit Transfers with Locally Optimal Control Laws", Journal of Spacecraft and Rockets, Vol. 44, No. 1, 2007, pp 273 – 276.

13 Bate, R.R., Mueller, D.D., White, J.E., "Fundamentals of Astrodynamics", Dover Publications, New York, 1971, pp. 385 – 387.

14 Walker, M.J.H., Ireland, B., Owens, J., "A Set of Modified Equinoctial Elements", Celestial Mechanics, Vol. 36, 1985, pp. 409-419.

15 Betts, J. T., "Optimal Interplanetary Orbit Transfers by Direct Transcription", Journal of Astronautical Sciences, Vol. 42, No. 3, July-Sept. 1994, pp 247-268.

16 Dormand, J.R., Price, P.J., "A Family of Embedded Runge-Kutta Formulae", Journal of Computing and Applied Mathematics, Vol. 6, 1980, pp 19 – 26.

17 Walker, M.J.H., Ireland, B., Owens, J., "A Set of Modified Equinoctial Elements", Celestial Mechanics, Vol. 36, 1985, pp. 409-419.

18 Betts, J. T., "Optimal Interplanetary Orbit Transfers by Direct Transcription", Journal of Astronautical Sciences, Vol. 42, No. 3, July-Sept. 1994, pp 247-268.

19 Becerra, V.M., "Solving complex optimal control problems at no cost with PSOPT", Proceedings of the IEEE Multi-conference on Systems and Control, Yokohama, Japan, September 2010, pp. 1391-1396.